Experiment-based motion reconstruction and restitution coefficient estimation of a vibro-impact system

Tao Li, Sébastien Seguy, Claude-Henri Lamarque, Alain Berlioz

Tao Li[1]
SinoMed LifeTech (Shenzhen) Co., Ltd.,
1505, Block T2, Ali Center,
Shenzhen 518054, Nanshan District, China
e-mail: li_tao_lumiere@126.com

Sébastien Seguy
ICA (Institut Clément Ader), CNRS,
INSA, ISAE, UPS, Mines Albi,
Université de Toulouse,
3 rue Caroline Aigle,
Toulouse F-31077, France
e-mail: seguy@insa-toulouse.fr

Claude-Henri Lamarque
École Nationale des Travaux Publics de l'État,
LTDS UMR CNRS 5513,
Université de Lyon,
3 rue Maurice Audin,
Vaulx-en-Velin Cedex 69518, France
e-mail: claude.lamarque@entpe.fr

Alain Berlioz
ICA (Institut Clément Ader), CNRS,
INSA, ISAE, UPS, Mines Albi,
Université de Toulouse,
3 rue Caroline Aigle,
Toulouse F-31077, France
e-mail: alain.berlioz@univ-tlse3.fr

Experiment-Based Motion Reconstruction and Restitution Coefficient Estimation of a Vibro-Impact System

The objective of this paper is to demonstrate the motion reconstruction and the parameter estimation of a vibro-impact (VI) system from limited experimental information. Based on the measured displacement and acceleration of its linear main system, the rest motion information such as the displacement and velocity of the attached VI energy sink can be calculated rather than difficult direct measurement, and therefore, different response regimes from the strongly modulated response to the classic regime with two impacts per cycle are reconstructed. Consequently, it provides comprehensive experimental data for the validation of analytical and numerical results and for any experimental bifurcation analysis. Moreover, a procedure to estimate the restitution coefficient from periodic impacts is demonstrated. This new experimental approach to estimate the value of the restitution coefficient is simple and this accurate value could play an important role in analytical and numerical study. [DOI: 10.1115/1.4041367]

1 Introduction

Recently, the vibro-impact (VI) phenomenon with energy transfer and dissipation at the impact moments is extensively studied in the framework of targeted energy transfer [1,2].

The recent advance from the further studies by Lee et al. [3] and Gendelman [4–6]. The former finds special orbits that are responsible for efficient energy transfer. The latter concentrates on the response with two impacts per cycle, no matter permanent or intermittent, since it is related to resonance captures. Before their researches, there have been some studies [7,8], especially in the experimental aspect.

Later, a series of research about the VI nonlinear energy sink (NES) is carried out from an experimental viewpoint [9–15]. Although these experiments are carried out for different objectives, they have some common characteristics and therefore they are analyzed as a whole.

First, the existence of two impacts per cycle, no matter in strongly modulated response with the strong modulation of displacement amplitude and intermittent impacts or in resonance with permanent two impacts per cycle, is the essence and proved to be relevant to efficient vibration control [12–14]. Second, only partial motion information is measured because of the limit of measure device. In most cases, only the displacement and acceleration of the main system are recorded, but the motion of the impact ball is difficult to measure and consequently unknown. Third, there exists a gap between experimental results and numerical results. For example, although a same optimal design mechanism for targeted energy transfer [16] is observed from both

numerical and experimental results in Ref. [12], there exists a value shift for the selection of design parameters. This situation is not only observed in recent study results but also ubiquitous for former researches with experimental validations [17]. The main reason is the neglect of some factors like friction and inclination, especially the inaccurate measure of restitution coefficient. Therefore, the purpose of this paper is to solve these encountered problems during the former studies, namely to reconstruct the whole motion from limited experimental data and to explain the gap between different results obtained from different study methods.

There are at least three models of restitution coefficient that describe three aspects of motion [18], namely, kinematic form by Newton, kinetic form by Poisson and energetic form by Stronge. The one developed by Newton is widely applied during the analytical treatment of system with vibro-impact. To obtain reliable analytical and numerical results, the precise value of restitution coefficient is of fundamental importance.

Thus, the objective of this paper is double, namely, to reconstruct the motion of a nonlinear system with vibro-impact and to explore a simple approach to estimate parameters from experimental results, especially the restitution coefficient.

The paper is organized as follows: In Sec. 2, the model of a vibro-impact system is presented. In Sec. 3, the configuration and experimental results are introduced. In Sec. 4, the reconstruction of different motion regimes is introduced. In Sec. 5, an approach to estimate restitution coefficient and its corresponding results are presented. Finally, Sec. 6 concludes the paper.

2 Prototype of Vibro-Impact and Modeling

A vibro-impact prototype with a ball inside a clearance of a linear oscillator (LO) is widely studied to simulate the complicated impact phenomenon as shown in Fig. 1. This model is the same as that has been used to study its nonlinear dynamics and damper
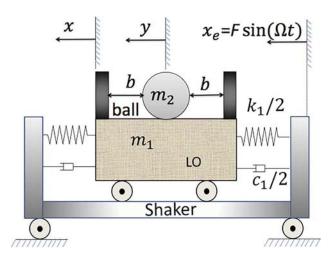
Fig. 1 Schema of a LO coupled with a VI NES under periodic excitation

characteristic in Refs. [9,11,12]. LO is periodically driven by a shaker, and the friction between LO and the ball (VI NES) that is neglected in the former studies will be considered here, but it will only be simply treated with just a little analytical development and experimental analysis.

Between impacts, the system is governed by the following equation:

$$m_1\ddot{x} + c_1(\dot{x} - \dot{x}_e) + k_1(x - x_e) + \alpha f_0 = 0$$
$$m_2\ddot{y} = \alpha f_0 \qquad (1)$$
$$\forall |x - y| < b$$

where

$$f_0 = \mu m_2 g \qquad (2)$$

and x, m_1, c_1, and k_1 are the displacement, mass, damping, and stiffness of LO, respectively. y and m_2 are the displacement and mass of VI NES, respectively. Dots denote differentiation with respect to time t. b represents the clearance. $x_e = F\sin(\Omega t)$ is the displacement imposed on the base by the shaker. f_0 represents the force contribution by dynamic friction between ball and LO, and μ is the dynamic friction coefficient. The sign of f_0 is denoted by α and always has the opposite sign compared to $\dot{y} - \dot{x}$.

After the following parameters are introduced

$$\varepsilon = \frac{m_2}{m_1}, \quad \omega_0{}^2 = \frac{k_1}{m_1}, \quad \tau = \omega_0 t$$
$$\lambda = \frac{c_1}{m_2\omega_0}, \quad \Omega = \frac{\omega}{\omega_0}, \quad G = \frac{F}{\varepsilon} \quad f_1 = \frac{f_0}{m_1}$$

we obtain the following dimensionless form:

$$\ddot{x} + \varepsilon\lambda\dot{x} + x + \alpha f_1 = \varepsilon G\sin\Omega\tau + \varepsilon^2\lambda G\Omega\cos\Omega\tau$$
$$\varepsilon\ddot{y} = \alpha f_1 \qquad (3)$$
$$\forall |x - y| < b$$

where $\varepsilon G\sin\Omega\tau$ and $\varepsilon^2\lambda G\Omega\cos\Omega\tau$ represent the contribution of force by the displacement and velocity of shaker, respectively. Here, dots denote differentiation with respect to dimensionless time τ.

When $|x - y| = b$, impacts occur. The relation between after and before impact is obtained under the hypothesis of simplified shock theory developed by Newton and the condition of momentum conservation

$$x^+ = x^-, \quad y^+ = y^-$$
$$\dot{x}^+ + \varepsilon\dot{y}^+ = \dot{x}^- + \varepsilon\dot{y}^-, \quad \dot{x}^+ - \dot{y}^+ = -r(\dot{x}^- - \dot{y}^-) \qquad (4)$$
$$\text{for } |x - y| = b$$

where r is the restitution coefficient, and the superscripts $+$ and $-$ indicate time immediately after and before impact.

Here, an underlying hypothesis is that the restitution coefficient will be the same at two sides of LO during all time, and will not be influenced by other parameters like velocity. Although this treatment can greatly simplify the analytical treatment [9], this
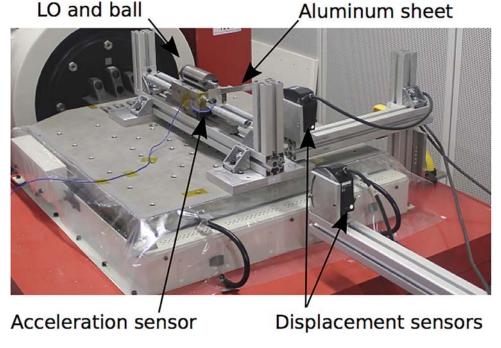

Fig. 2 Experimental configuration of an LO coupled with a VI NES (ball)
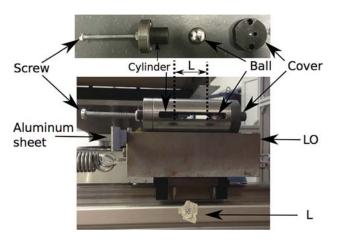
Fig. 3 Detailed view of an LO and a VI NES

Table 1 Parameters of the experiment [11]

Physical parameters			
m_1	4.168 kg	c_1	3.02 Ns/m
k_1	11.47×10^3 N/m	m_2	32 g
b	11.5 mm		
Reduced parameters			
ε	0.76%	λ	1.80

assumption is not perfectly verified in practice and it introduces some errors as will be presented in the following analysis.

3 Experiment Introduction

An experimental configuration is presented in Fig. 2. A shaker can generate periodic excitation with fixed amplitude (0.5 mm) and frequency (8 Hz) to control LO through four linear springs. Within a clearance of LO, a ball can move freely inside and impacts two sides of LO. A detailed view of LO and VI NES is shown in Fig. 3. These two sides of LO are in different situations. The right part is made of hardened steel and totally fixed. On the contrary, the left side can be regulated by a cylinder that is made of hardened steel and fixed to a screw. In this way, clearance $b = L/2$ can be adjusted.

Here, only the acceleration of LO, displacement of LO and shaker are recorded by sensors. The actual sensitivity of displacement and acceleration sensor is 10,000 mV/mm and 50.34 mV/g, respectively. The sample frequency is 6400 Hz and the length of measure time is 5.12 s for all tests. Actually, the displacement of

LO is indirectly measured from the displacement of aluminum sheet by a laser sensor. The velocity or displacement of ball is not measured because of the limit of measure device.

Experimentally obtained parameters are shown in Table 1. Then the value of L ($2b$) is changed to observe its influence on the response regimes and bifurcation routes. Because only partial information can be obtained, the nonlinear dynamics is only characterized from the impact time difference in Ref. [11]. This time, if the motion of VI NES can be reconstructed from the limited information, the complex nonlinear dynamics of this vibro-impact system can be further analyzed from more viewpoints.

4 Motion Reconstruction

In this section, the objective is to demonstrate the procedure to reconstruct the motion of the whole system for different values of the clearance b. We first explain the motion reconstruction for $b = 9$ mm.

Its time history of acceleration is shown in Fig. 4. When no VI NES is attached, there would be no impact and the acceleration of LO should be a smooth sine curve. When VI NES is added, there is an addition of a transient impulse for each impact. Here, all impacts are marked by crosses. As a result, impact time can be obtained. Overall, the impact strengths reflected in the acceleration of LO are constant though with fluctuation. Then their distribution is further analyzed.

As has been done for other clearances in Ref. [10], two consecutive impact time differences are used to construct a point, and two such consecutive points are used to construct a vector, and all vectors of this time history of acceleration are applied to construct the first return map of impact time difference as shown in Fig. 5. A line means two asymmetrical impacts per cycle.

Then its time history of displacement is shown in Fig. 6, and impact moments are marked out and represented by red circles. For any two consecutive impacts, the following conditions should hold:

$$\begin{aligned}|x(t_i) - y(t_i)| = b \\ (x(t_i) - y(t_i))(x(t_{i+1}) - y(t_{i+1})) < 0\end{aligned} \quad (5)$$

where t_i is the ith impact time, $x(t_i)$ and $y(t_i)$ are the displacement of LO and VI NES at impact moments, respectively.

Here, the displacement of VI NES at the impact moments can be calculated. If the friction between LO and VI NES can be neglected, the whole time history of displacement of VI NES can be estimated as represented by dotted curve in Fig. 7. The time history of LO is shifted to the negative and positive direction by b, respectively, to better demonstrate the reconstructed displacement of VI NES. As a result, one impact moment denoted by one circle (A0) is shifted to a point in the positive side (A1) and
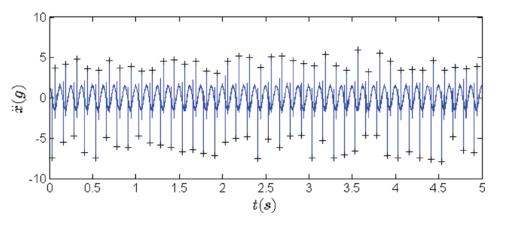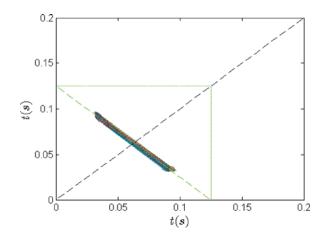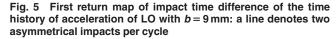

Fig. 4 Acceleration of LO with $b = 9$ mm: impact moments are denoted by crosses

Fig. 5 First return map of impact time difference of the time history of acceleration of LO with $b = 9$ mm: a line denotes two asymmetrical impacts per cycle

another point in the negative side (A2). Evidently, there is just a point among them will be connected to the displacement of VI NES as shown in Fig. 7. Therefore, the motion of the whole system is reconstructed this time.

Then we do the same thing for other response regimes with other clearances, namely, $b = 15$ mm and $b = 17.5$ mm.

The time history of acceleration of LO with $b = 15$ mm is shown in Fig. 8, its intermittent and irregular characteristic with two impacts per cycle is well demonstrated by the irregular distribution of impact time. With the same procedure, its motion is reconstructed as shown in Fig. 9.

Then, for $b = 17.5$ mm, its time history of acceleration and constructed time history of displacement are displayed in Figs. 10 and 11, respectively.

In addition to these three typical clearances, other responses with other clearances can also be reconstructed such as $b = 7.5$ mm and 6 mm, etc. Based on the experimentally obtained information, other analysis such as bifurcation analysis can be continued. However, the objective here is just to present the possibility to identify full experimental information, and further
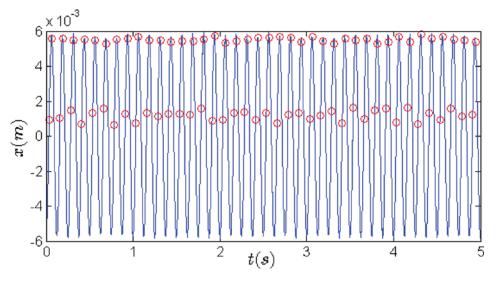

Fig. 6 Displacement of LO with $b = 9$ mm: impact moments are denoted by circles
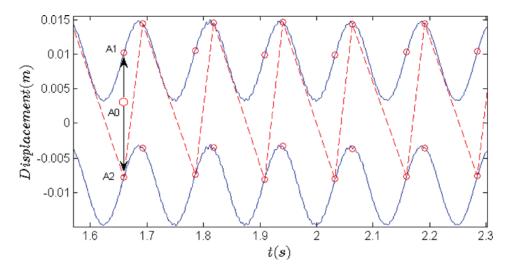

Fig. 7 Reconstruction of the displacement of VI NES in dotted curve with $b = 9$ mm: displacement of LO in sine curve is shifted to negative and positive by b, and impact moments are denoted by circles
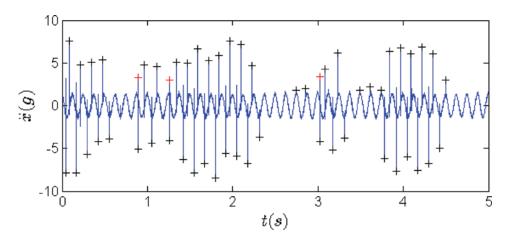
Fig. 8 Acceleration of LO with $b = 15$ mm: impact moments are denoted by crosses [10]
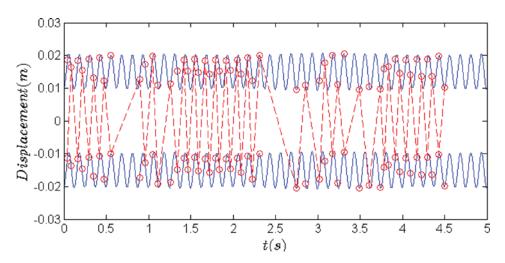

Fig. 9 Reconstruction of the displacement of VI NES in dotted curve with $b = 15$ mm: displacement of LO in sine curve is shifted to negative and positive by b and impact moments are denoted by circles

analysis based on the obtained information is not the subject of this paper, though it is rare and worth doing.

5 Restitution Coefficient Estimation

In this section, we continue the analysis of the results with $b = 9$ mm in order to estimate the restitution coefficient.

The velocity $\dot{y}_i$ of VI NES between ith and $(i+1)$th impact is constant regardless of friction and inclination and can be calculated through the following relation:

$$y(t_{i+1}) - y(t_i) = \dot{y}_i \Delta t_{i+1}$$
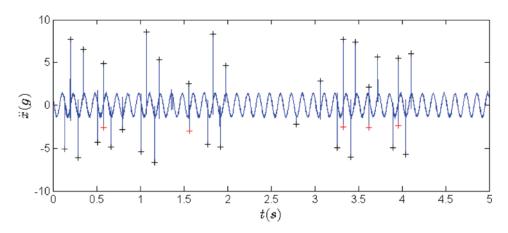$$\Delta t_{i+1} = t_{i+1} - t_i \tag{6}$$

Fig. 10 Acceleration of LO with $b = 17.5$ mm: impact moments are denoted by crosses
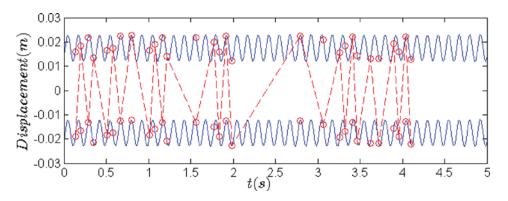
Fig. 11 Reconstruction of the displacement of VI NES in dotted curve with $b = 17.5$ mm: displacement of LO in sine curve is shifted to negative and positive by b and impact moments are denoted by circles
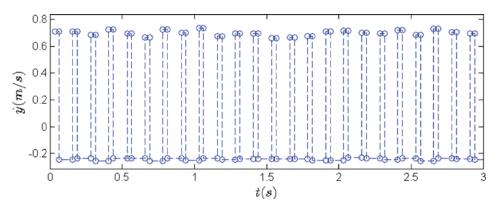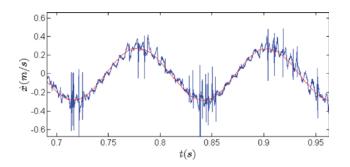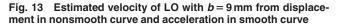

Fig. 12 Velocity of VI NES with $b = 9$ mm: impact moments are denoted by circles

Fig. 13 Estimated velocity of LO with $b = 9$ mm from displacement in nonsmooth curve and acceleration in smooth curve
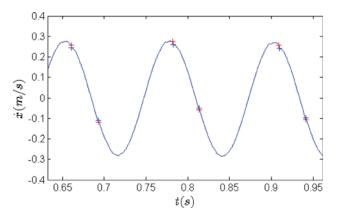

Fig. 14 Velocity of LO before and after impact in crosses with $b = 9$ mm
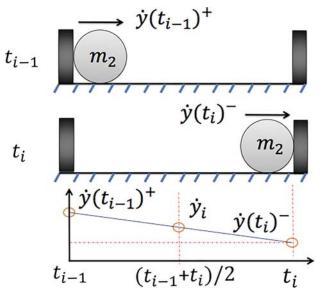

Fig. 15 Schema of corrected velocities after and before impacts

Therefore, velocity of VI NES can be calculated as shown in Fig. 12. Its two velocities at different directions are almost constant and alternate from one to another.

To estimate the velocity of LO, there are two ways, namely from time history of displacement and acceleration, respectively. The results estimated from the former are shown by nonsmooth curve in Fig. 13 and the results from the latter are represented by smooth curve. The impact information should be reflected by sudden changes of velocity in the time history of velocity, but it is
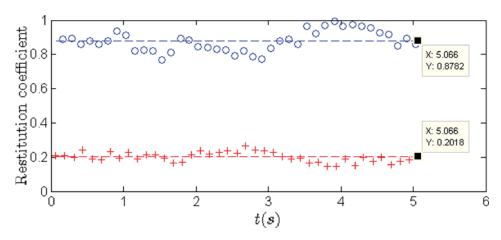
Fig. 16 Estimated restitution coefficients at the right side in circles and the left side in crosses with $b = 9$ mm: dotted lines are two corresponding values of root-mean-square

Table 2 Influence of dynamic friction coefficient μ

| M | Restitution coefficient | |
	Right side	Left side
0	0.8782	0.2018
0.09	0.8769	0.2003
0.2	0.8752	0.1984
0.4	0.8721	0.195
0.6	0.8691	0.1916

totally lost in nonsmooth curve. In addition, there exist higher frequency components, which are supposed to result from the vibration of aluminum sheet during the measure process as shown in Figs. 2 and 3.

The velocities of LO before impact ($\dot{x}^-$) and after impacts ($\dot{x}^+$) are marked out in crosses in Fig. 14. Here, just a part of time history is shown and if the view is enlarged enough, these two different moments can be clearly distinguished. Of course, there may exist errors because of sample frequency, but errors should be very small, since the recorded data can represent the abrupt process of change.

If dynamic friction is considered, velocities of VI NES after impact time t_{i-1} and before impact time t_i should be corrected as shown in Fig. 15.

Specifically, the value of dynamic friction is as follows:

$$f_0 = \mu m_2 g \qquad (7)$$

where μ is dynamic friction coefficient and the sign of friction f_0 is always adverse to the relative velocity between VI NES and

LO. Then, the following velocities before impact and after impact can be obtained according to the average velocity $\dot{y}_i$ of VI NES between two consecutive impact times t_{i-1} and t_i:

$$\dot{y}(t_{i-1})^+ = \dot{y}_i + f_0 \Delta t_i / 2$$
$$\dot{y}(t_i)^- = \dot{y}_i - f_0 \Delta t_i / 2 \qquad (8)$$
$$\Delta t_i = t_i - t_{i-1}$$

Then, restitution coefficient at an impact moment t_i can be calculated through the following equation:

$$r_i = -\frac{\dot{y}(t_i)^+ - \dot{x}(t_i)^+}{\dot{y}(t_i)^+ - \dot{x}(t_i)^-} \qquad (9)$$

where $\dot{y}(t_i)^-$ and $\dot{y}(t_i)^+$ are two velocities of VI NES before and after the ith impact. Similarly, $\dot{x}^-$ and $\dot{x}^+$ are velocities of LO before and after the ith impact.

At first, no friction is considered and the estimated restitution coefficient is shown in Fig. 16. The circles and crosses correspond to the restitution coefficients at the right and left side of LO as shown in Fig. 3. Since the left side is a mass fastened to a screw, there are many possible situations. In one respect, it may not be firmly fixed initially, and it may become loose during the experiment process in another respect. Because of the same reason, its fastened level may be different for each clearance. These phenomena are already observed during the experiment process. It probably results in the low value of coefficient restitution and great changes of coefficient restitution at the left side for different clearances. Of course, there may exist other reasons that should be further explored, e.g., the difference of impact velocity.
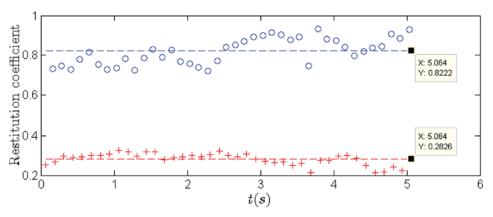

Fig. 17 Estimated restitution coefficients at the right side in circles and the left side in crosses with $b = 7.5$ mm: dotted lines are two corresponding values of root-mean-square
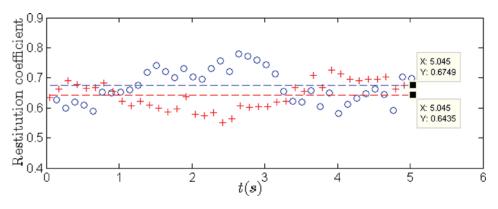
Fig. 18 Estimated restitution coefficients at the right side in circles and the left side in crosses with *b* = 6 mm: dotted lines are two corresponding values of root-mean-square

Then friction is considered and μ is chosen between [0.09, 0.6]. The estimated root-mean-square of restitution coefficient does not change much for this interval of μ as shown in Table 2. It means that velocity is large enough and the change of velocity caused by friction can be neglected. Therefore, the estimated restitution coefficient with $\mu = 0$ as shown in Fig. 16 is reliable. However, the selection of μ will play an important role in the estimation of restitution coefficient for response with $b = 17.5$ mm, since the velocity of VI NES at this case is low. Correspondingly, it is not recommended to estimate restitution coefficient from that case or similar cases.

Then I calculate the restitution coefficient for other two clearances still with two asymmetrical impacts per cycle, namely $b = 7.5$ mm and 6 mm. The results are shown in Figs. 17 and 18, respectively. Evidently, the estimated restitution coefficient changes as the change of clearance. The main difference is the change of impact velocity resulting from different clearances. Since the objective in this paper is to provide a method to estimate restitution coefficient, the influence of other parameters will not be further analyzed here.

6 Conclusion

This paper is devoted to the motion reconstruction and parameter estimation of a vibro-impact system from limited experimental data. First, its impact model and corresponding experimental results are introduced. Then, the motion reconstruction is carried out from limited experimental data. Finally, the restitution coefficients are estimated.

Based on the partial experimental data of LO, a procedure is proposed to reconstruct different response regimes, from strongly modulated response to regimes with two impacts per cycle. Then, the constructed information of motion can be used not only to validate analytical and numerical results but also to further analyze the nonlinear dynamics from the experimental viewpoint.

Moreover, the restitution coefficient is a fundamental parameter in the domain of impact. Although there are some approaches to measure its value, it is still not so easy. The method applied in this paper is an approach by repetitive impacts and it is seldom used. It is observed that this approach is rather simple and can be applied for other purposes that need the acquisition of the restitution coefficient as a prerequisite. Two such purposes are common, namely to study the influence of parameters on the restitution coefficient and to apply the restitution coefficient for the study of nonlinear dynamics of vibro-impact systems. Although many details are simplified during the modeling of the motion of the ball, it does not influence much on the effect of the proposed approach to estimate the value of restitution coefficient.

References

[1] Ibrahim, R. A., 2009, *Vibro-Impact Dynamics: Modeling, Mapping and Applications*, Vol. 43, Springer Science & Business Media, Berlin.
[2] Vakakis, A. F., Gendelman, O., Bergman, L., McFarland, D., Kerschen, G., and Lee, Y., 2008, *Nonlinear Targeted Energy Transfer in Mechanical and Structural Systems*, Vol. 156, Springer Science & Business Media, Berlin.
[3] Lee, Y., Nucera, F., Vakakis, A., McFarland, D., and Bergman, L., 2009, "Periodic Orbits, Damped Transitions and Targeted Energy Transfers in Oscillators With Vibro-Impact Attachments," Physica D, **238**(18), pp. 1868–1896.
[4] Gendelman, O. V., 2012, "Analytic Treatment of a System With a Vibro-Impact Nonlinear Energy Sink," J. Sound Vib., **331**(21), pp. 4599–4608.
[5] Gendelman, O., and Alloni, A., 2015, "Dynamics of Forced System With Vibro-Impact Energy Sink," J. Sound Vib., **358**, pp. 301–314.
[6] Gendelman, O., and Alloni, A., 2016, "Forced System With Vibro-Impact Energy Sink: Chaotic Strongly Modulated Responses," Procedia IUTAM, **19**, pp. 53–64.
[7] Nucera, F., Vakakis, A. F., McFarland, D. M., Bergman, L. A., and Kerschen, G., 2007, "Targeted Energy Transfers in Vibro-Impact Oscillators for Seismic Mitigation," Nonlinear Dyn., **50**(3), pp. 651–677.
[8] Nucera, F., Lo Iacono, F., McFarland, D. M., Bergman, L. A., and Vakakis, A. F., 2008, "Application of Broadband Nonlinear Targeted Energy Transfers for Seismic Mitigation of a Shear Frame: Experimental Results," J. Sound Vib., **313**(1–2), pp. 57–76.
[9] Gourc, E., Michon, G., Seguy, S., and Berlioz, A., 2015, "Targeted Energy Transfer Under Harmonic Forcing With a Vibro-Impact Nonlinear Energy Sink: Analytical and Experimental Developments," ASME J. Vib. Acoust., **137**(3), p. 031008.
[10] Li, T., Seguy, S., and Berlioz, A., 2016, "Dynamics of Cubic and Vibro-Impact Nonlinear Energy Sink: Analytical, Numerical, and Experimental Analysis," ASME J. Vib. Acoust., **138**(3), p. 031010.
[11] Li, T., Seguy, S., and Berlioz, A., 2017, "On the Dynamics Around Targeted Energy Transfer for Vibro-Impact Nonlinear Energy Sink," Nonlinear Dyn., **87**(3), pp. 1453–1466.
[12] Li, T., Seguy, S., and Berlioz, A., 2017, "Optimization Mechanism of Targeted Energy Transfer With Vibro-Impact Energy Sink Under Periodic and Transient Excitation," Nonlinear Dyn., **87**(4), pp. 2415–2433.
[13] Li, T., Gourc, E., Seguy, S., and Berlioz, A., 2017, "Dynamics of Two Vibro-Impact Nonlinear Energy Sinks in Parallel Under Periodic and Transient Excitations," Int. J. Nonlinear Mech., **90**, pp. 100–110.
[14] Li, T., Qiu, D., Seguy, S., and Berlioz, A., 2017, "Activation Characteristic of a Vibro-Impact Energy Sink and Its Application to Chatter Control in Turning," J. Sound Vib., **405**, pp. 1–18.
[15] Pennisi, G., Stephan, C., Gourc, E., and Michon, G., 2017, "Experimental Investigation and Analytical Description of a Vibro-Impact Nes Coupled to a Single-Degree-of-Freedom Linear Oscillator Harmonically Forced," Nonlinear Dyn., **3**(3), pp. 1769–1784.
[16] Wei, Y., Peng, Z., Dong, X., Zhang, W., and Meng, G., 2017, "Mechanism of Optimal Targeted Energy Transfer," ASME J. Appl. Mech., **84**(1), p. 011007.
[17] Bapat, C., and Sankar, S., 1985, "Single Unit Impact Damper in Free and Forced Vibration," J. Sound Vib., **99**(1), pp. 85–94.
[18] Ahmad, M., Khairul Azwan, I., and Mat, F., 2016, "Impact Models and Coefficient of Restitution: A Review," ARPN J. Eng. Appl. Sci., **11**(10), pp. 6549–6555.